THE EUROPEAN SOCIETY OF MEDICINE
Medical Research Archives, Volume 13 Issue 6

RESEARCH ARTICLE

The Use of Optical Coherence Tomography Imaging and Vibrational Studies to Compare Noninvasive Measurements and Histopathology: A pilot Study of Squamous Cell Carcinoma

Gayathri Kollipara[1], Frederick H. Silver[1,2*], Tanmay Deshmukh[2], and Aanal Patel[1]

[1]Department of Pathology and Laboratory Medicine, Robert Wood Johnson Medical School, Rutgers, the State University of New Jersey, Piscataway, NJ 08854, USA.
[2]OptoVibronex, LLC., Ben Franklin Tech Ventures, Bethlehem, PA 18105, USA.

[*]silverfr@rutgers.edu

OPEN ACCESS

PUBLISHED
30 June 2025

CITATION
Kollipara, G., Silver, F.H., et al., 2025. The Use of Optical Coherence Tomography Imaging and Vibrational Studies to Compare Noninvasive Measurements and Histopathology: A pilot Study of Squamous Cell Carcinoma. Medical Research Archives, [online] 13(6). https://doi.org/10.18103/mra.v13i6.6543

COPYRIGHT
© 2025 European Society of Medicine. This is an open- access article distributed under the terms of the Creative Commons Attribution License, which permits unrestricted use, distribution, and reproduction in any medium, provided the original author and source are credited.

DOI
https://doi.org/10.18103/mra.v13i6.6543

ISSN
2375-1924

ABSTRACT

Background: Squamous cell carcinoma is a cutaneous skin lesion that is the second numerous skin cancer after basal cell carcinoma. It is more likely to metastasize to secondary sites compared to basal cell carcinomas.

Objective: To determine if noninvasive optical coherence tomography images and vibrational data can be correlated with histopathology of squamous cell carcinoma to better understand how this lesion can be determined without a biopsy.

Methods: We have used vibrational optical coherence tomography and histopathology to determine if optical coherence tomography subchannel images and noninvasive measurements can be correlated with lesion histopathology. Optical tomography images were collected on cancer excisions before they were sent for standard diagnosis by a dermatopathologist. The gray scale optical coherence tomography images were broken down into green (low pixel intensity), blue (medium intensity), and red (high intensity) subchannels images and scanned to create pixel intensity versus depth plots. Quantitative mechanovibrational spectra and optical coherence tomography images during vibration with sound frequencies between 50 and 80 Hz were also collected.

Results: Our results indicate that green subchannel maximum pixel intensities representing the cellular content of squamous cell carcinomas are lower than those of normal skin and appear to decrease as the lesion size of keratinous accumulations increase. In addition, the blue subchannel which provides information on collagen appears to change as the size and amount of the lesions increases. This is due to the forward scattering (Mie scattering) of the infrared light deeper into the sample by the large cellular and keratin accumulations present.

Conclusion: The height and width of the pixel intensity versus depth plots can be used to characterize the type of lesion and its relative size. In addition, when the sample is vibrated at or near the resonant frequency of the cancer associated fibroblasts (CAFs) and keratinocytes the lesion almost vanishes in the green, blue, and red subchannels channels. These results suggest that vibrational coherence tomography can be used in telemedicine to classify lesions in areas where Dermatologist visits are difficult to schedule.

Keywords: VOCT, OCT, squamous cell cancer, imaging, resonant frequency, elastic modulus, RGB subchannel images

Introduction

Approximately 5.4 M BCCs and squamous cell cancers (SCCs) are diagnosed in the US each year; about 8 out of 10 of these cancers are BCCs [1], of which 60-80% are reported to be the nodular type[2]. The remaining skin cancers are SCCs. Diagnostic evaluation of skin cancer is done primarily by visual inspection and dermoscopy. Dermoscopy is the most widely used method to detect skin cancers since they are characterized by several morphological characteristics. BCCs typically present clinically as pearly, shiny, smooth nodules with small dilated, branched blood vessels that can ulcerate or bleed[1]. Dermoscopic diagnostic criteria for pigmented BCCs have been well documented[3,4]. While dermoscopic diagnostic criteria are quite diverse, based on recent VOCT studies the physical properties of different types of BCCs are similar[5]. Characteristics of SCC include white circles, white structureless areas, keratin pearls, and a polymorphous vascular pattern[6].

Nonmelanoma skin cancer (NMSC) is the most common form of skin cancer in the Caucasian population, with squamous cell carcinoma (SCC) accounting for the majority of NMSC metastases and deaths[1]. It is believed that actinic keratosis (AK) a UV-induced lesion in the skin can eventually transform into a cancerous lesion termed squamous cell cancer (SCC). AK and SCC have a similar genetic profile, including alterations in the p53 gene. The estimated annual risk of progression from AK to SCC is small; however, the cumulative risk for a patient with multiple AK lesions over time is substantial[2]. Squamous cell carcinoma (SCC), has one of the highest incidences of all cancers in the United States, is an age-dependent disease primarily on patients over 70 years of age[3]. Recent evidence suggests that dermal wounding therapies, can decrease the proportion of senescent dermal fibroblasts, increase dermal IGF-1 expression, thus protecting geriatric keratinocytes from UVB-induced SCC initiation [3]. Tobacco smoke and alcohol drinking are major risk factors for squamous cell carcinoma of the head and neck. The mean level of apoptotic capacity in the SCC cases was reported to be significantly lower than that in the control patients who did not smoke or drink alcohol[4].

Ultraviolet-induced P53 mutations are early events in cancer stroma cells (CSCs), and are responsible for great genomic instability[5]. Other genetic changes occur in CDKN2A and NOTCH and in oncogenes, such as RAS[5]. Mouse models of squamous cell carcinoma (SCC), have demonstrated that tumor cells responding to transforming growth factor β (TGF-β) function as drug-resistant cancer stem cells (CSCs). The gene expression of TGF-β–responding tumor cells has accelerated the identification of the pathways that CSCs drive invasive tumor progression[7]. DEK, a conserved nuclear factor, has been reported to play important roles in the progression of early and late-stage SCC[8].

Histologically, typical SCC is characterized by nests of squamous epithelial cells arising from the epidermis and extending into the dermis. The malignant cells are often large with abundant eosinophilic material when stained with H&E. Keratin pearls form when malignant epithelial cells, which have lost their cohesion, become arranged concentrically, and then undergo keratinization[8].

In this pilot study we compare SCC histopathology of two patient cases with noninvasive data obtained using OCT and vibrational analysis to correlate data determined noninvasively with histopathology.

Methods

OCT Image Collection

The Vibrational OptoScope used in this study consisted of a Lumedica OQ 2.0 OCT (Lumedica Inc, Durham,NC) equipped with a small 2.0 inch speaker as described previously operating at a wavelength of 840 nm collecting 13,000 frames per second[9-11]. The measurements were made in vivo on intact control skin and in vitro and on excised SCC biopsies. All images were made as part of IRB approved clinical studies on skin at Rutgers Center for Dermatology as discussed previously[9]. Clinical diagnoses were made by a board certified dermatopathologist after H&E staining and review of the tissue sections as part of routine clinical skin excisional protocols. Raw image OCT data were collected and processed using MATLAB software and image J[9-11]. All OCT images were created by scanning the skin or SCC cross section. The gray scale scans were color coded using image j as reported previously[9]. Pixel intensity versus depth plots were generated by scanning the gray scale OCT images parallel to the

surface of the samples[9]. The OCT gray scale pixel images were also broken into green, blue, and red subchannel images using a lookup table as reported previously[9]. By breaking up the pixel intensity distribution at each point into low (green), medium (blue), and high (red) intensities, it is possible to examine differences in reflection of the different layers of skin and skin lesions.

VOCT Measurements

The OQ Labscope 2.0 was modified by adding a 2 inch-diameter speaker placed about 2.0 inches from the tissue to be vibrated in the VOCT studies[9-11]. A sinusoidal sound wave at 55 dB was produced using an app supplied by the I5 computer that is part of the Labscope. Both the sound wave and the light were applied to the surface along the axis of the light beam. The deflection of the surface along the direction of the light beam was measured. All weighted displacement measurements were made from line data at a single point based on the location of the lesion using the OCT lesion image[9]. The Labscope was modified to collect and store single raw image data that were used to calculate sample displacements (amplitude information) from A line data. The data were processed using MATLAB software, as discussed previously[9-11]. The displacement of the tissue in phase with the sound was detected by measuring the frequency dependence of the tissue deformation based on the reflected infrared light. The reflected light was filtered to collect only vibrations that were in-phase (elastic component) with the sound input signal. The amplitude of the displacement was plotted against the frequency of the vibrations. The result is a spectrum of displacements (mechanovibrational spectrum) for specific tissue components as a function of the frequency of the applied sound; the resonant frequency of each tissue component, e.g., cells (50–80 Hz), dermal collagen (100–120 Hz), blood vessels (130–150 Hz), and fibrotic tissue (180–260 Hz), have been assigned previously based on studies on a variety of soft tissues[9-11].

Results

In this study we collected OCT images and histopathology on a small SCC and a large SCC to determine if OCT and histological images could be correlated. Figure 1A shows a color-coded OCT image of normal skin. The various colors include the stratum corneum (yellow), the germinating cell layers (pink and red), and the blue are generated by the reflections from the papillary dermal layer. The image in Figure 1A is broken into low (Figure 1B, green), medium (Figure 1C, blue), and high (Figure 1D, red) subchannel pixel intensity images providing details about the different layers found in the sample. The corneocytes are found in the green layer (B), the hyporeflective portion of the blue layer are reflections are from the keratin intermediate filaments while the blue layer also reflects light from the papillary dermis seen in blue. The red image (D) contains information on all layers except the stratum corneum. Note the presence of a hair follicle in A, C, and D (black vertical line) which is also hyporeflective.

© 2025 European Society of Medicine

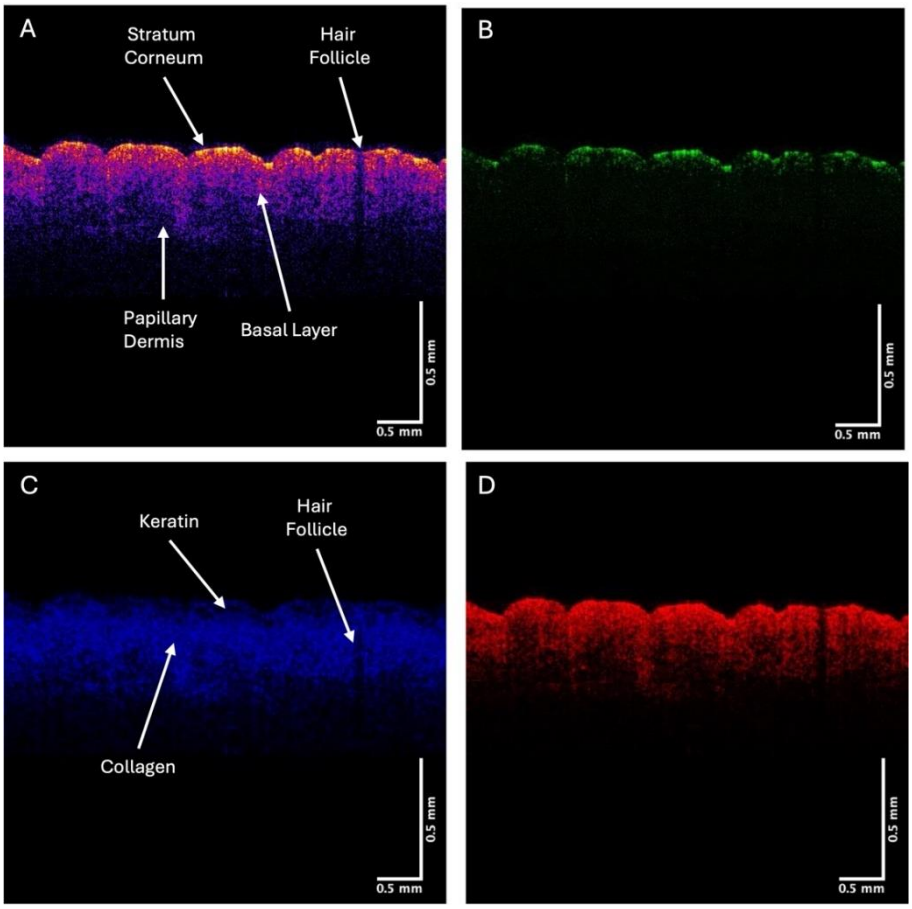

Figure 1. An OCT image of color-coded (A), green (B), blue (C), and red (D) subchannel images of normal skin. Note the arrows pointing to the hyporeflective region (1C) in normal skin consistent with the keratin intermediate filaments present in the cells of the mid epidermis. Keratin in hair in the skin is also hyporeflective as is shown in Figure 1A. The green, blue, and red subchannel images are shown in Figure 1B, C, and D.

The OCT images can be scanned to give quantitative data on the pixel intensities as a function of depth to provide details concerning the location of cells, keratin, and collagen in the OCT images. Figure 2 shows a weighted displacement versus frequency plot (mechanovibrational spectrum) for VOCT studies on normal skin. Note the cellular resonant frequencies are seen at about 60 Hz +/- 10 Hz (normal cells), 100 Hz (papillary dermal collagen), 150 Hz (normal blood vessels), and 250 Hz and above (reticular dermal collagen) [9-11]. Note the mechanovibrational spectrum of normal skin is dominated by the papillary collagen signal.

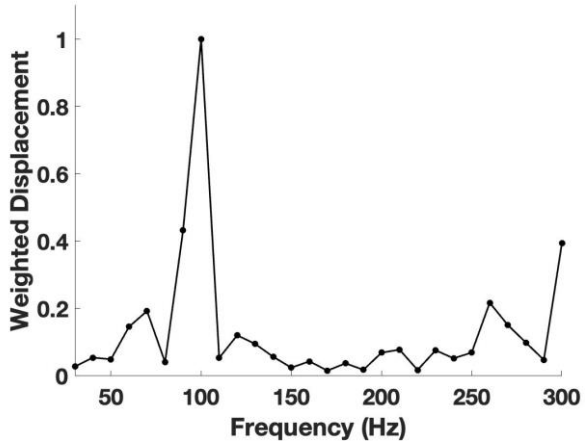

Figure 2. A typical plot of weighted displacement versus frequency (mechanovibrational spectrum) obtained from VOCT studies on normal skin. Cellular resonant frequencies are seen at about 60 Hz +/-10 Hz (normal cells), collagen at 100 Hz (papillary dermal collagen), and 260 Hz (reticular collagen). Note the mechanovibrational spectrum of normal skin is dominated by the dermal collagen signal[9-11].

© 2025 European Society of Medicine

Typical plots of pixel intensity versus depth for normal skin (A), the green (B), blue (C), and red (D) subchannels are shown in Figure 3. The green subchannel (B) contributes to the image at a depth of the stratum corneum, the blue channel (C) contributes maximally to the germinating and papillary layers, and the red channel (D) is seen throughout the depth of the skin but does not appear to show the stratum corneum.

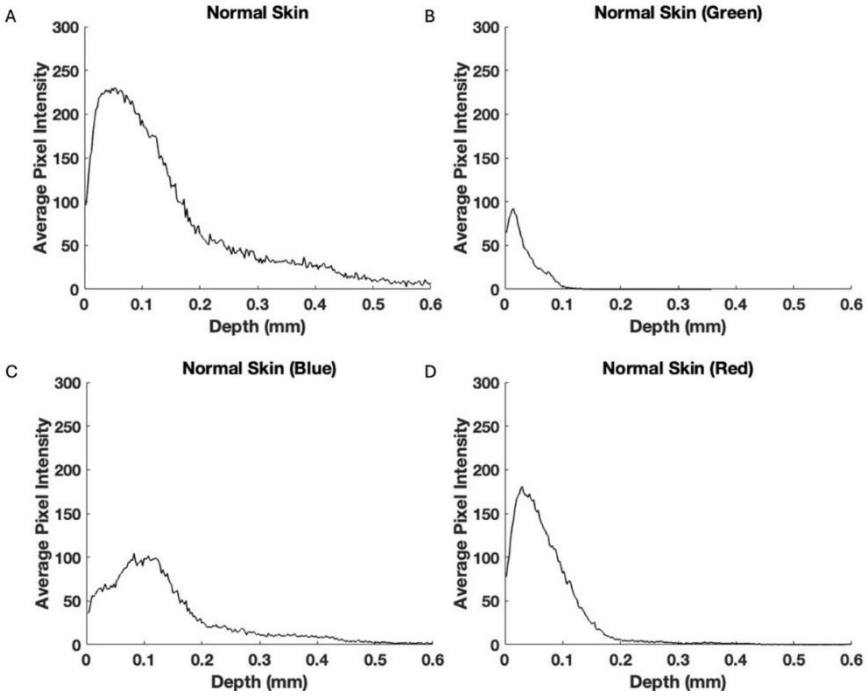

Figure 3. Typical plots of pixel intensity versus depth for normal skin (A), the green (B), blue (C), and red (D) subchannels. The blue subchannel shows an inflection point at about 0.05 mm, which may be due to reflections from the interface between keratin-producing cells in the granulating region and the beginning of the papillary dermis. Note the red subchannel appears to provide information on reflections from the green and blue subchannels in the skin.

Figure 4A shows the histopathology of a lesion diagnosed as SCC by a dermatopathologist. The color-coded OCT images are shown in Figures B, while the green (C), blue (D), and red (E) subchannels are also shown. One of the cancerous lesions is circled in Figures 4A, B, C and D. Note the area where the lesion is found in 4A shows reduced reflection in the green channel (4B) as well as a loss of the hyporeflective region (4D). The red arrow points to the hyporeflective region in 4D that is missing in the area where the lesion is.

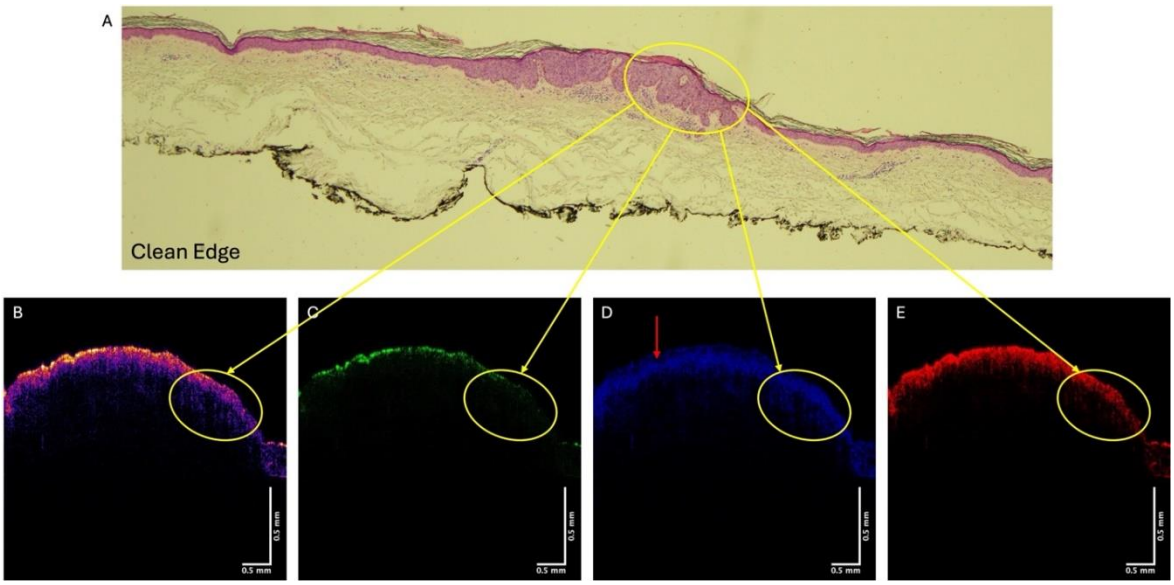

Figure 4. Histopathology (A), OCT color-coded image (B), green (C), blue (D), and red (E) subchannel images of a SCC from patient 29. Note the hyporeflective region in D (red arrow) that putatively represents microfilament keratin seen in normal epidermis is missing in D where the lesion is circled.

© 2025 European Society of Medicine

When the sample is vibrated at frequencies between 50 and 80 Hz the image changes in its intensity.

Figure 5 illustrates the OCT images of color-coded, and subchannel images of the SCC from patient 29 during vibration at 50, 60, 70, and 80 Hz. Note the lesion image (see circled region) partially disappears when vibrated at 70 and 80 Hz.

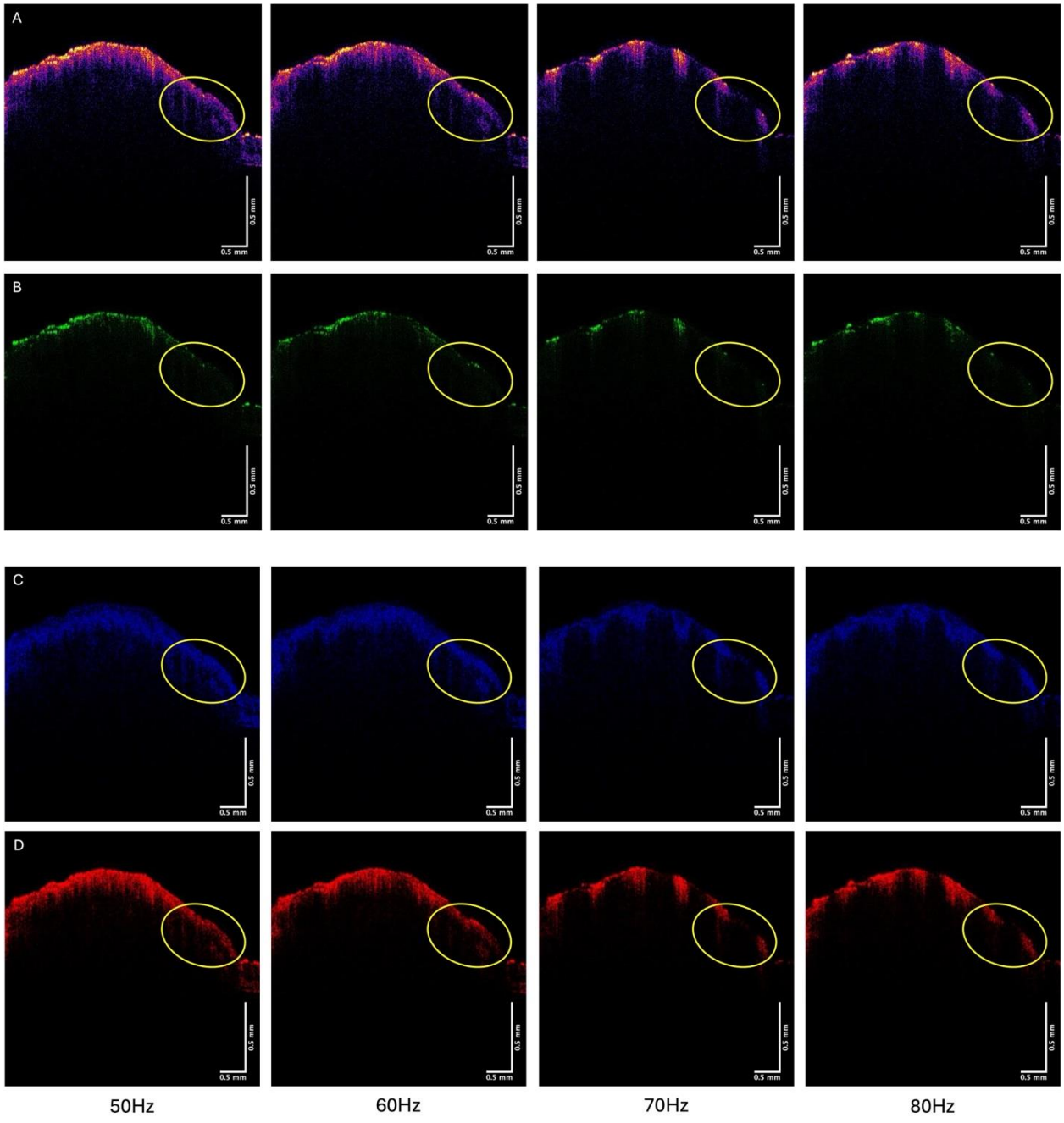

Figure 5. OCT images of SCC from Patient 29 from Figure 4 vibrated at 50, 60, 70 and 80 Hz for color-coded (A), green (B), blue (C), and red (D) subchannels. The circled region image disappears in the green subchannel and loses intensity in the blue and red subchannels when vibrated at 70 and 80 Hz.

Figure 6 shows that the average pixel intensity versus depth plot (left) obtained by scanning the SCC from patient 29 parallel to the surface and the weighted displacement versus frequency (right) generated by vibrating the sample between frequencies of 30 and 300 Hz. Normal skin has resonant frequency peaks at 50 Hz (cells), 100 Hz (dermal collagen), and 150 Hz (blood vessels) [10-12]. Cancerous lesions have new peaks at about 80 Hz (cancer associated fibroblasts (CAFs) and keratinocytes), 130 Hz (new thin blood vessels), and 250-260 Hz (fibrotic tissue) [9-11]. The new peaks at 80, 130, and 260 Hz in Figure 6 are indicative of a cancerous lesion.

© 2025 European Society of Medicine

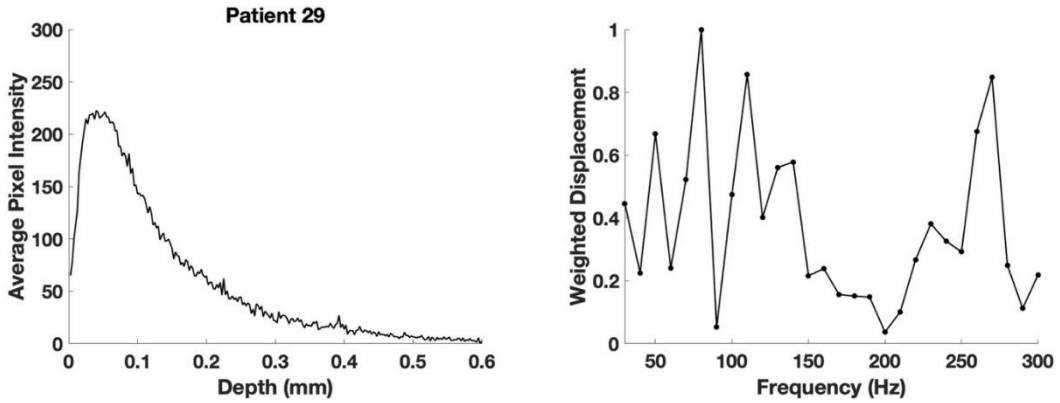

Figure 6. Pixel intensity versus depth (left) for the color-coded image and weighted displacement versus frequency (right) for the SCC from patient 29 shown in Figure 4B. The pixel intensity of the reflected light falls off with increased depth of the sample because of both Rayleigh (small particles) and Mie scattering (large particles) of the light. Note the new peaks at 80, 130, and 260 Hz are indicative of cancerous tissues[9-11] .

Figure 7 shows plots of pixel intensity versus depth for the SCC from patient 29. The green subchannel maximum height previously reported for normal skin is about 100[9-11] compared to a value of about 65 for the SCC from patient 29 shown in Figure 7.

The blue subchannel width reported previously for normal skin is generally shifted to the right in SCC[9]. The red subchannel for the SCC seen in Figure 7 is also shifted to the right compared to that reported for normal skin as shown in Figure 3.

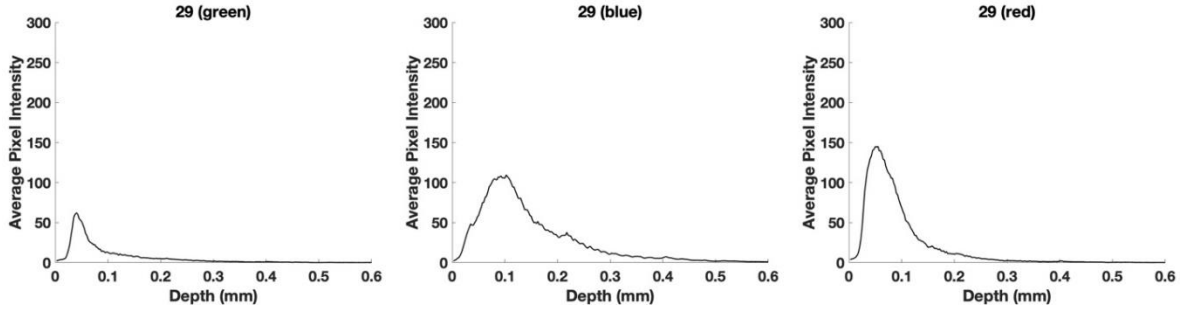

Figure 7. Pixel intensity versus depth for green (A), blue (B), and red (C) subchannels of images shown in Figure 1C, D, and E. Note that the green channel is lower than that of normal skin and the blue and red channels appear shifted to the right because of Mie scattering by SCC cell-tissue aggregates.

In comparison to the small lesion, Figure 8 shows histopathology and OCT images for a large SCC from patient 23. The lesion circled in the histopathology (8A) is also circled in the color-coded OCT (Figure 8B) and the images of the green (8C), blue (8D), and red (8E) subchannels. Note there are other lesions that are not circled in the histopathology that are found in Figure 8 to avoid confusion.

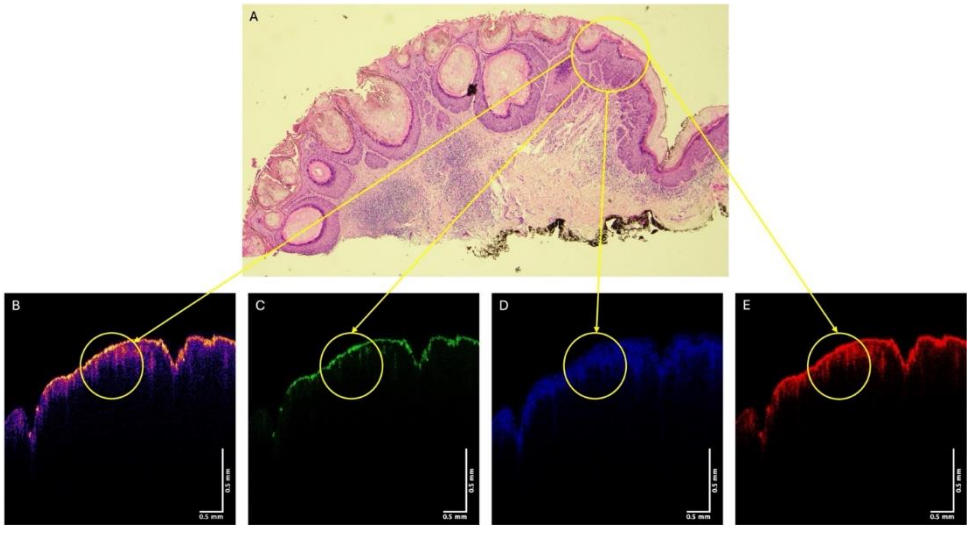

Figure 8. Histopathology of a SCC from Patient 23 (A) and color-coded OCT image (B), green (C), blue (D), and red (E) subchannel images. Note the circled region in A contains what appears to be keratin deposits. There are many lesions not circled in Figure 8A to avoid confusion.

Figure 9 shows the color-coded OCT image of the SCC from patient 23 (A), and the green (B), blue (C), and red (D) subchannel images during vibration at 50, 60, 70, and 80 Hz. Note the lesion seen in Figure 8A is circled in the images in Figure 9. Note the lesion circled in Figure 9 partially disappears when vibrated at 70 and 80 Hz, especially in the green channel. Other lesions seen in Figure 9A also disappear when vibrated at 70 and 80 Hz.

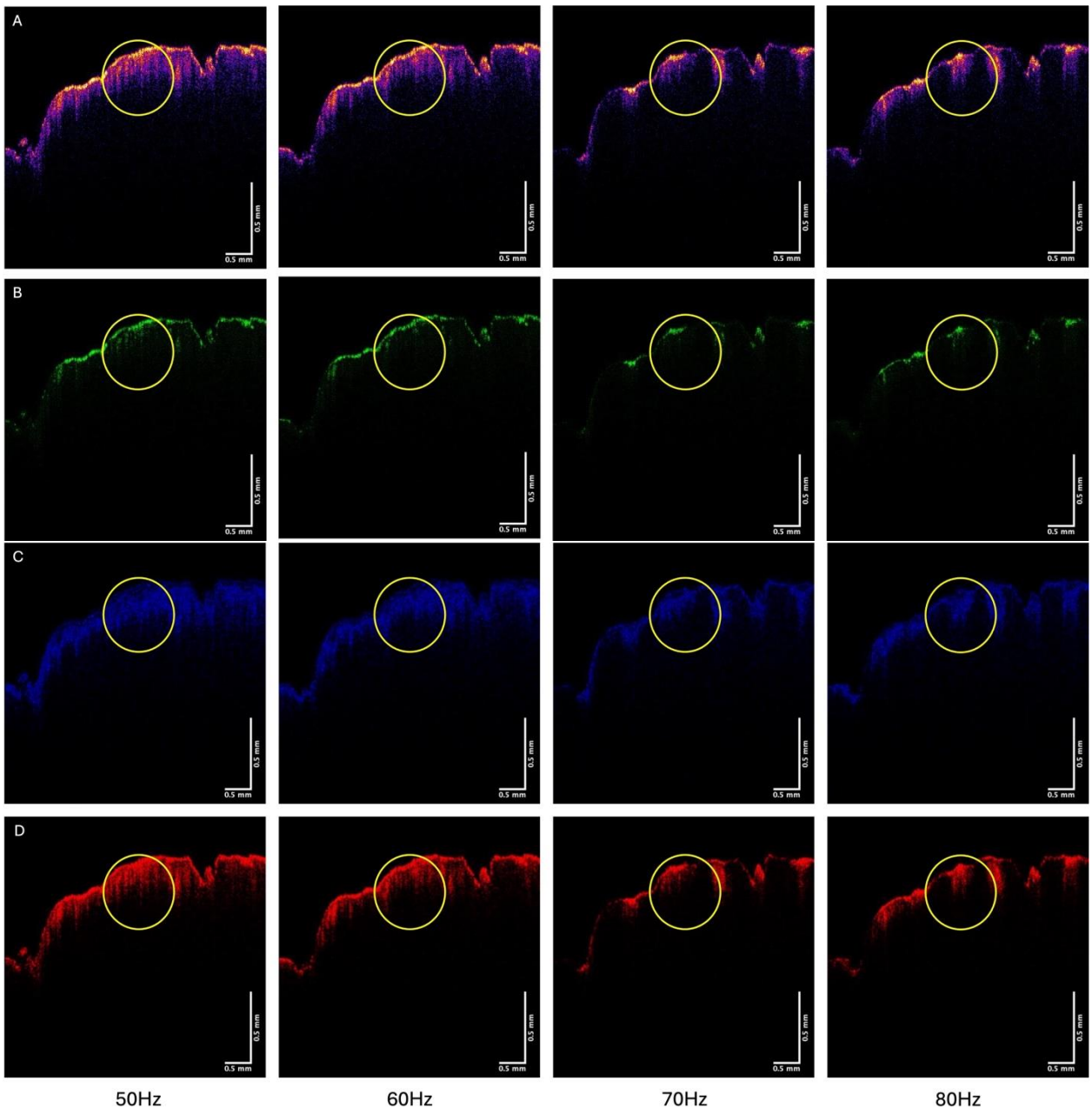

Figure 9. Color-coded OCT images of SCC during vibrations at 50, 60, 70 and 80 Hz for patient 23 (A), and green (B), blue (C), and red (D) subchannel images during vibration. Note the circled lesion appears to partially disappear in the green channel image at 70 and 80 Hz as well as other lesions that are seen in Figure 5A.

Figure 10 shows a plot of pixel intensity versus depth (left) and a plot of weighted displacement versus frequency (right) for the SCC from patient 23. Note the pixel intensity versus depth plot is somewhat broader than that for patient 23 (Figure 3) compared to that for patient 29. The weighted displacement versus frequency plot for patient 23 shows a large peak at 80 Hz and a smaller one at 250-260 Hz compared to that for patient 29 (Figure 3).

© 2025 European Society of Medicine

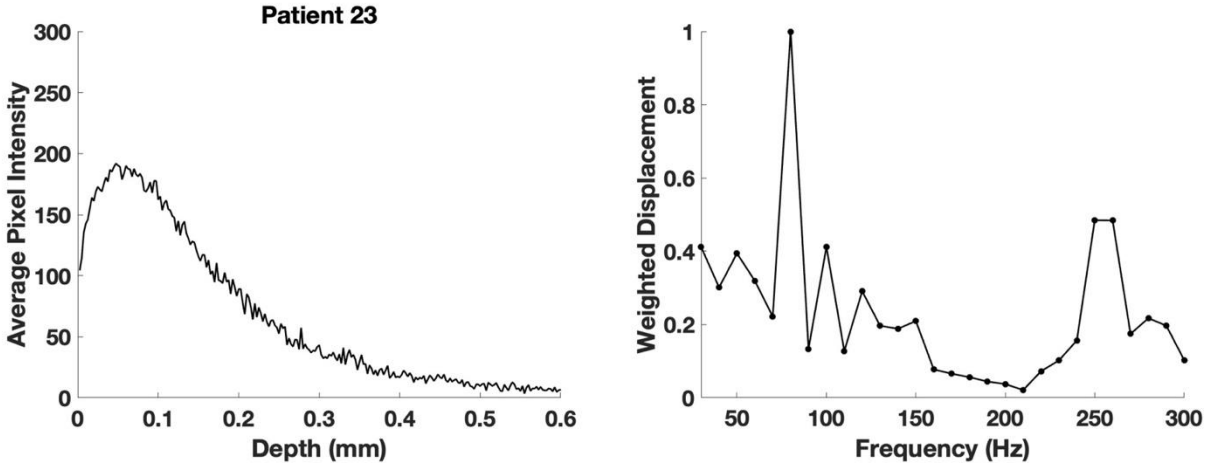

Figure 10. Average pixel intensity versus depth for color-coded image (left) and weighted displacement versus frequency (right) for the SCC shown from patient 23. Note the increased width of the pixel intensity versus depth plot compared to Figure 3. The resonant frequency peaks at 80, 130, and 250-260 Hz are indicative of a cancerous lesion[9-11].

Figure 11 shows plots of pixel intensity versus depth for the SCC from patient 23 and weighted displacement versus depth (right) for the color-coded and subchannel images. Note the green subchannel pixel maximum height is about 45 which is lower than that for patient 29 and that for normal skin[9-11]. The lower green channel height is likely due to forward scattering by the large keratin deposits seen in the histopathology image of patient 23 due to elastic scattering (Mie scattering).

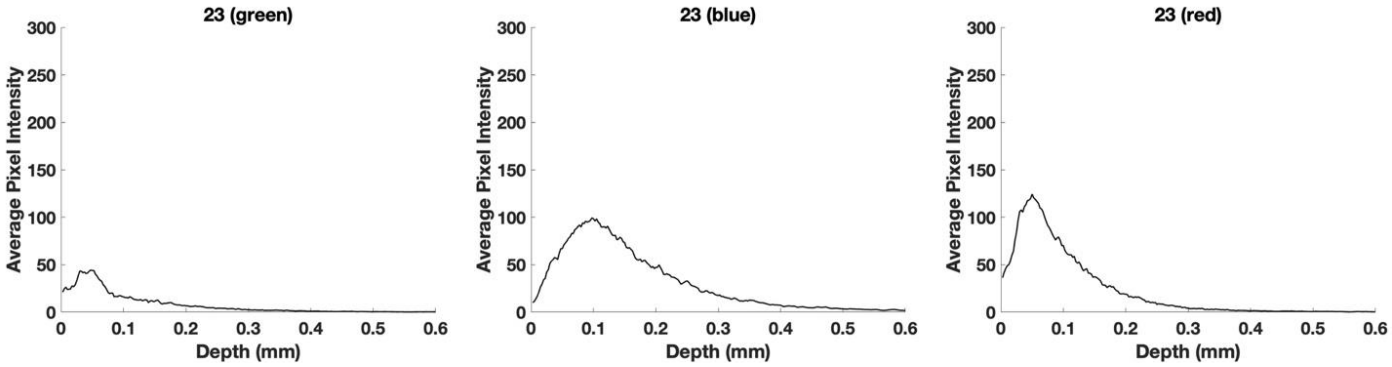

Figure 11. Pixel intensity versus depth for green (A), blue (B), and red (C) subchannels of images shown in Figure 8C, D, and E. The low value of the maximum pixel maximum intensity for the green subchannel appears to be due to Mie scattering by the large keratin deposits in the SCC from patient 23.

Discussion

Differentiation of normal skin from benign lesions and cancerous tissue has been a major diagnostic challenge as the number of skin cancers continues to increase worldwide. Yet, rapid early diagnosis of small lesions is important to provide a wider array of treatment options. Excisional versus topical treatments have become important issues especially for keratinocyte cancers. Depending on their size, shape, and rate of recurrence there maybe different treatment options[12,13] While identification of suspicious lesions can be achieved based on visual and dermoscopic analysis, identification of lesion subtype can be further refined based on other imaging methods including ultrasound and vibrational optical coherence tomography, based on their size and shape[14]. Skin malignancies are the most common type of cancer diagnosed in the United States (US) and the number of Dermatologist visits are increasing each year. The clinical diagnosis of SCC remains a challenge for most primary care physicians (PCPs), to whom initial presentations usually occur[15,16]. Recently, the use of an elastic scattering device was approved by the FDA to be used by primary care physicians (PCPs) to improve diagnostic and management sensitivity by correctly classifying most benign lesions of patient concern. This may increase skin cancer detection while improving access to specialist care[17].

The DermaSensor™, an FDA approved device is a handheld, wireless, and battery powered unit that emits pulses of light at various wavelengths, that illuminates tissue and records the backscattered optical reflectance of the tissue. The output of the device produces a lesion classification that provides the practitioner with information that can be used to develop a treatment plan for cancerous lesions[17].

The limitation of this device is that it does not provide the practitioner with a lesion image that can be directly correlated with the histopathology, nor does it provide quantitative physical properties that can be used to characterize the lesion. We have developed a technique called vibrational optical coherence tomography (VOCT) that combines imaging and vibrational analysis to noninvasively quantitatively characterize skin lesions. The use of VOCT to image and analyze the resonant frequency and elastic modulus of the components of benign and malignant skin lesions has been reported previously[9-11]. The technique provides direct images of cancerous lesions that can be correlated with the diagnoses made by a dermatopathologist.

In this study we compare histopathology and OCT images of small and large SCCs in an attempt to show the relationship between noninvasive OCT images, physical data, and histopathology. The results of this limited study indicate that both SCCs exhibit similar behaviors to basal cell carcinomas (BCCs). The lesion subchannel images show different infrared light reflective properties due to reduction in the infrared light reflections by cell and tissue aggregates especially in the green and blue subchannels. In addition, when the cancerous areas of the lesions are vibrated at 60, 70, or 80 Hz the lesion images reduce in intensity and can be visually identified on the color coded subchannel images as hyporeflective regions.

Light is absorbed, scattered, and reflected when it interacts with tissues with different water and macromolecular components. In skin, infrared light is partially reflected and scattered by the components of the epidermis and dermis[9]. Scattering of light by tissues occurs by small (Raleigh) and large particles (Mie). In cancerous tissues, when nodules or clusters of cells and/or large macromolecular complexes form such as collagen in fibrotic tissues and keratin in pearls, the light is forward scattered deeper into the tissues[9]. This results in changes in the pixel intensities and distribution of pixels as a function of sample depth.

The results of this study suggest that OCT images collected noninvasively can provide information on the size and reflective properties of lesions from patients diagnosed with SCCs. Green subchannel maximum pixel intensities of SCCs are lower than those of normal skin and decrease as the lesion size increases. In addition, the blue subchannel is displaced to the right as size increases. This is due to the forward scattering (Mie scattering) of the infrared light deeper into the sample by the large cellular and keratin aggregates present. Therefore, the height and width of the pixel intensity versus depth plot can be used to characterize the type of lesion and its relative size. In addition, when the sample is vibrated at or near the resonant frequency of the CAFs and keratinocytes (70 and 80 Hz) the lesion almost vanishes in the green, blue, and red subchannels channels. It is possible by vibrating dense lesions at their resonant frequency they condense and this limits light reflection.

The heights of 80, 130, and 250-260 Hz peaks are quite different for the small and large SCCs. The height of the 80 Hz peak is highest in the large SCC suggesting that the amount of CAFs and keratinocytes increase compared to other peaks as the lesion gets larger. The 50 Hz peak all but disappears, indicating that the normal epithelial cells are replaced by cells associated with the growing cancer. This results in the deposition of keratin and keratin pearls that contribute to the 250-260 Hz peak. We have previously reported that although BCCs, SCCs, and melanomas all have 80, 130, and 250-260 Hz peaks not present in normal skin the ratio of the peak heights can be used to differentiate these cancers from each other and from benign lesions[11] and the pixel intensity versus depth plots provide specificities and sensitivities that range from about 80 to 90%[9].

The use of VOCT to screen patients noninvasively can be done remotely with only the need for a technician to focus the image on the patient. This will allow skin screening in remote areas where dermatologists are in short supply and provide screening by general practitioners who are more abundant than Dermatologists.

Limitations to the study include the analysis of only two of the many SCCs that we have collected both

VOCT data and histopathology. Further studies are needed to extend these studies to lesions with more complicated histopathology to confirm the results.

Conclusions

We have compared OCT images and histopathology of 2 SCCs.OCT images collected noninvasively provide information on the size and reflective properties of these lesions. Green subchannel maximum pixel intensities of SCCs are lower than those of normal skin and may decrease as the lesion size and amounts of keratinous aggregates increase. In addition, the blue subchannel appears to change as the size and amount of the lesions increases. This is due to the forward scattering (Mie scattering) of the infrared light deeper into the sample by the large cellular and keratin particles present. The height and width of the pixel intensity versus depth plot can be used to characterize the type of lesion and its relative size. In addition, when the sample is vibrated at or near the resonant frequency of the CAFs and keratinocytes (70 and 80 Hz) the lesion almost vanishes in the green, blue, and red subchannels. This provides a mode by which more than one part of the lesion can be viewed at the same time when there are multiple cancerous parts.

The use of VOCT to screen patients noninvasively requires only a technician to focus the image on the patient. This will allow skin screening by telemedicine in remote areas where Dermatologists are in short supply. It can be used by general practitioners to screen patients.

Conflict of Interest Statement:

None.

Funding Statement:

None.

Acknowledgements:

None.

References:

1. Yanofsky VR, Mercer SE, Phelps RG. Histopathological variants of cutaneous squamous cell carcinoma: a review. *J Skin Cancer.* 2011;210813. doi: 10.1155/2011/210813.

2. Fernandez Figueras MT. From actinic keratosis to squamous cell carcinoma:pathophysiology revisited *JEADV* 2017; 31 (Suppl. 2): 5–7.DOI: 10.1111/jdv.14151

3. Travers JB, Spandau DF, Lewis DA, Machado C, Kingsley M, Mousdicas N, Somani AK. Fibroblast senescence and squamous cell carcinoma: how wounding therapies could be protective. *Dermatol Surg*. 2013;39(7):967-73. doi: 10.1111/dsu.12138.

4. Liu Z, Liu H, Han P, Gao F, Dahlstrom KR, Li G, et al. Apoptotic Capacity and Risk of Squamous Cell Carcinoma of the Head and Neck. *Eur J Cancer*. 2017; 72: 166–176. doi:10.1016/j.ejca.2016.11.018.

5. Corchado-Cobos R, García-Sancha N, González-Sarmiento R, Pérez-Losada J, Cañueto J. Cutaneous Squamous Cell Carcinoma: From Biology to Therapy. *Int J Mol Sci*. 2020;21(8):2956. doi: 10.3390/ijms21082956.

6. Sgouros D, Theofili M, Damaskou V, Theotokoglou S, Theodoropoulos K, Stratigos A, Theofilis P, Panayiotides I, Rigopoulos D, Katoulis A. Dermoscopy as a Tool in Differentiating Cutaneous Squamous Cell Carcinoma From Its Variants. *Dermatol Pract Concept*. 2021;11(2):e2021050. doi: 10.5826/dpc.1102a50.

7. Oshimori N. Cancer stem cells and their niche in the progression of squamous cell carcinoma. *Cancer Sci.* 2020;111(11):3985-3992. doi: 10.1111/cas.14639.

8. Ishida K, Nakashima T, Shibata T, Hara A, Tomita H. Role of the DEK oncogene in the development of squamous cell carcinoma. *Int J Clin Oncol*. 2020;25(9):1563-1569. doi: 10.1007/s10147-020-01735-5.

9. Silver, F.H.; Deshmukh, T.; Patel, A.; Dhillon, J.; Bobra, A.; Nadiminti, H.*; British Journal of Cancer Research.* 2025, 8(1), 747- 755. doi: 10.31488/bjcr.2025.

10. Silver, F.H.; Deshmukh, T.; Patel, A.; Nadaminti, H. Use of Optical Coherence Tomography Images to Differentiate Between Normal Skin, Skin Lesions, and Melanoma: A Pilot Study. *Journal of Cancer Science and Therapy.* 2024;16:06.

11. Silver, F.H.; Deshmukh, T.; Ryan, N.; Romm, A.; Nadiminti, H."Fingerprinting" Benign and Cancerous Skin Lesions Using Vibrational Optical Coherence Tomography: Differentiation among Cancerous Lesion Types Based on the Presence of New Cells, Blood Vessels, and Fibrosis. *Biomolecules* 2022;12:1332.doi.org/10.3390/biom12101332.

12. Shaw FM, Weinstock MA. Comparing Topical Treatments for Basal Cell Carcinoma. *J Invest Dermatol* 2018;138(3):484–486. doi:10.1016/jid.2017.11.024.

13. Neugebauer R, Su KA, Zhu Z, Sokil M, Chren MM, Friedman GD, *et al*. Comparative effectiveness of treatment of actinic keratosis with topical fluorouracil and imiquimod in the prevention of keratinocyte carcinoma: A cohort study. *J Am Acad Dermatol* 2019;80(4):998–1005.doi:10.1016/j.jaad.2018.11.024.

14. Halip IA, Vâţă D, Statescu L, Salahoru P, Patraşcu AI, Temelie OliniciD, *et al*. Assessment of Basal Cell Carcinoma Using Dermoscopy and High Frequency Ultrasound Examination. *Diagnostics* (Basel);12(3):735. doi:10.3390/diagnostics12030735.

15. Tepedino M, Baltazar D, Hanna K, Bridges A, Billot L, Zeitouni NC. Elastic Scattering Spectroscopy on Patient-Selected Lesions Concerning for Skin Cancer*. The Journal of the American Board of Family Medicine* 2024; 37 (3): 427-435; doi: https://doi.org/10.3122/jabfm.2023.230256R2.

16. Jaklitsch E, Thames T, de Campos Silva T, Coll P, Oliviero M, Ferris LK. Clinical Utility of an AI-powered, Handheld Elastic Scattering Spectroscopy Device on the Diagnosis and Management of Skin Cancer by Primary Care Physicians. *J Prim Care Community Health*. 2023;14:21501319231205979. doi: 10.1177/21501319231205979.

17. Manolakos D, Patrick G, Geisse JK, Rabinovitz H, Buchanan K, Hoang P, et al. Use of an elastic-scattering spectroscopy and artificial intelligence device in the assessment of lesions suggestive of skin cancer: A comparative effectiveness study *JAAD International* 2024;14:52-58.